

DESIGN AND PROPERTIES OF A NEW DCCT CHAMBER FOR THE PF-RING AT KEK

R. Takai*¹, T. Honda¹, Y. Tanimoto¹, T. Nogami, T. Obina¹

High Energy Accelerator Research Organization (KEK), Tsukuba, Ibaraki, Japan

¹also at SOKENDAI (The Graduate University for Advanced Studies), Tsukuba, Ibaraki, Japan

Abstract

A DC current transformer (DCCT) for the PF-ring was renewed during the 2018 summer shutdown. A vacuum chamber for the new DCCT was designed based on a circular duct with an inner diameter of 100 mm and has a structure housing a toroidal core inside of electromagnetic shields. The geometry of the ceramic break for interrupting the wall current flow was optimized using a three-dimensional electromagnetic field simulator, and the break was fabricated considering some technical limitations. Both ends of the ceramic break were short-circuited in a high-frequency manner by a sheet-like capacitive structure to suppress the radiation of unneeded higher-order modes (HOMs) into the core housing. The ceramic break is also equipped with water-cooling pipes on metal sleeves brazed to the both ends to efficiently remove the heat generated by HOMs. The new DCCT chamber has been used already in user operation without any problems. A temperature rise near the ceramic break is still approximately 6 °C, even when a 50-mA isolated bunch is stored.

INTRODUCTION

In the Photon Factory storage ring (PF-ring), which is a dedicated light source of KEK, two DC current transformers (DCCTs) have been installed to measure the stored beam current in the ring [1]. It has been more than 20 years since the main DCCT for user operation was installed, and there is concern for failure due to aging. In addition, heat generation of the DCCT chamber caused by the higher-order modes (HOMs) emitted from the stored beam has become an issue for the filling pattern with a highly charged isolated bunch because the sectional shape of the chamber does not match the adjacent beam ducts. Because the stored current measured by the DCCT is one of the most important parameters in accelerator operation, we decided to update this old DCCT. For the toroidal core and signal-detection circuit of the components, an in-air model of the New Parametric Current Transformer (NPCT) and its electronics manufactured by Bergoz Instrumentation, which have been used successfully in many accelerators including the PF-ring, were adopted [2]. A vacuum chamber paired with the commercial core was designed and fabricated based on a circular duct with an inner diameter of 100 mm according to the duct shape at the installation site.

In this report, the detailed design of the new DCCT chamber with the ceramic break and its properties measured in different filling patterns are described.

DESIGN OF CERAMIC BREAK

To detect the electromagnetic field emitted from electron beams by the DCCT core placed outside of the beam duct, a part of the metal duct needs to be replaced by a ceramic to break the wall current flow accompanied with the beam propagation. However, because unneeded HOMs exceeding the measurement bandwidth of the DCCT are emitted into the core housing and can cause serious duct heating or electric discharges only by breaking the flow, both ends of this ceramic break are often short-circuited at high frequency by imparting an appropriate capacitance. The value of the capacitance C is determined by the cutoff frequency considering the measurement bandwidth and the impedance of the cavity structure formed by the core housing. For the core of the Bergoz Instrumentation, C is recommended to be set within the following range [3]:

$$10 \text{ nF} \leq C \leq 220 \text{ nF.} \quad (1)$$

In the case of DCCT chambers that have been used in the PF-ring, including the sub-DCCT, an alumina ceramic disk with a thickness of 0.5 mm is used as the ceramic break [4]. The ceramic disk has a hole corresponding to the adjacent duct shape at the center. Both sides of the disk are metalized, and a 0.5-mm-thick Kovar sleeve is brazed on each side. Such a structure where the thin ceramic disk is sandwiched between the metal sleeves is very effective for suppressing the duct heating because it is possible to reduce the beam-coupling impedance. However, because the outer diameter of the ceramic disk becomes much larger than that of the beam duct to realize the capacitance of the order of Eq. (1), there are some difficulties in manufacturing, cost, and handling. Therefore, a cylindrical ceramic break, which is also used in the Photon Factory Advanced Ring (PF-AR) and SuperKEKB (former KEKB) storage rings, was adopted for the new DCCT chamber [5]. In this method, the capacitance is secured by wrapping the exterior of the ceramic break with a sheet-like capacitive structure.

The beam simulation was conducted to evaluate the power loss generated when the beam propagated in a DCCT chamber by using a three-dimensional electromagnetic field simulator “GdfidL” [6]. Figure 1(a) shows a schematic layout of the simulated chamber model. The cylindrical ceramic break, whose longitudinal length is L and transverse thickness is T , is interposed in the middle of a circular duct

* ryota.takai@kek.jp

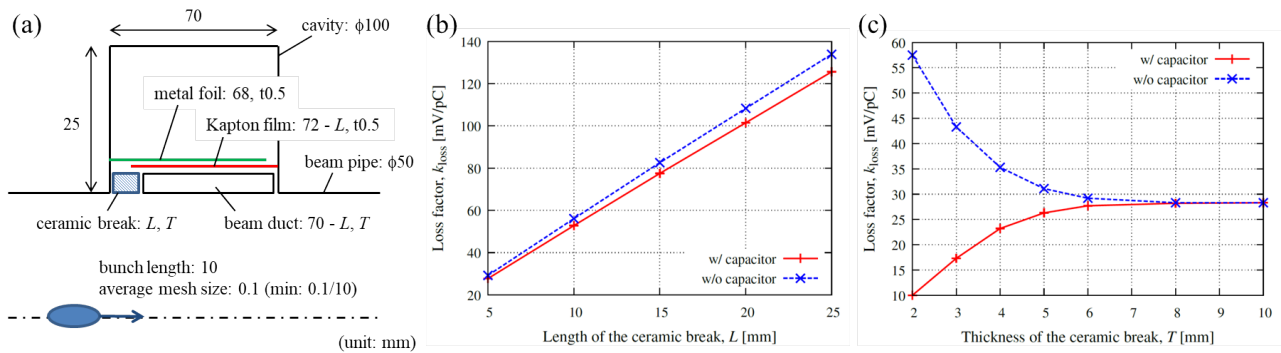


Figure 1: (a) Schematic layout of the DCCT chamber model used in the beam simulation (not to scale). Dependence of the loss factor on the (b) length and (c) thickness of the ceramic break.

with an inner diameter of 50 mm. The outside of the ceramic break is covered by a cavity space with an inner diameter of 100 mm and a longitudinal length of 70 mm. To simulate the capacitive structure described above, a conductive sheet insulated by a 500- μm -thick dielectric sheet is wrapped around the ceramic break and adjacent duct. One end of the conductive sheet on the ceramic break side is connected to the cavity wall to short circuit at high frequency between the ducts before and after the ceramic break through this capacitive structure. The relative permittivities of the ceramic break and dielectric sheet were set to 9.7 and 3.5 by assuming an alumina ceramic and Kapton film, respectively. The bunch length of the electron beam is set to 10 mm root mean square (RMS) by assuming the PF-ring. The average mesh size in the simulation is set to 100 μm in consideration of the thickness of the capacitive structure and the calculation time. By using such a simulation model, the relation between the dimensions of the ceramic break L , T and the loss factor k_{loss} induced when the beam propagates at the speed of light along the chamber axis was investigated.

Figure 1(b) shows the dependence of the loss factor on the length of the ceramic break. The thickness of the ceramic break was fixed to 6 mm. As shown in the figure, the loss factor grows proportionally with the length of the ceramic break. In addition, it is shown that the capacitive structure has an effect of reducing the loss factor by 5–6%.

Figure 1(c) shows the dependence of the loss factor on the thickness of the ceramic break. The length of the ceramic break was fixed to 5 mm. In cases with and without the capacitive structure, the loss factor decreases and increases rapidly as the ceramic break becomes thin, respectively. In either case, the loss factor converges to the same value in the range above the thickness of 8 mm. In other words, the capacitive structure is extremely effective in reducing the loss factor when the ceramic break is thin; otherwise, it has almost no effect.

From these simulation results, it is found that the shorter and thinner ceramic break with a capacitive structure is effective for suppressing the power loss caused when passing the beam. However, the technical limitations and influences

of machining on physical properties must also be considered when the ceramic break is actually manufactured. Accordingly, the length and thickness of the ceramic break were respectively determined to be 5 mm and 6 mm by considering actual conditions, such as the longitudinal withstand voltage, the stress strain generated by brazing, and the dimensional tolerance. The inner diameter of the ceramic break was set to 100 mm according to that of the beam duct. Because the roughness of the inner surface facing the beam can be a source of electric discharge, grinding after sintering was avoided. An etched metal coating on the inner surface to reduce the coupling impedance was also avoided for the same reason. Both end faces perpendicular to the beam axis were metalized and brazed with L-shaped sleeves made of Kovar.

The longitudinal coupling impedance calculated with the final dimensions, $L = 5$ mm and $T = 6$ mm, is shown in Fig. 2. An inner diameter of the cavity space was changed to 200 mm corresponding to the enlarged beam duct, while the other parameters were identical to those shown in Fig. 1(a). Although a periodic resonance structure is observed, the coupling impedance can be effectively suppressed by the effect of the capacitive structure. The loss factor for this model is calculated to be 14.4 mV/pC, and the power loss for each filling pattern adopted during user operation of the PF-ring is estimated as follows:

- Multibunch (250 bunches, 450 mA) : 7.3 W,
- Hybrid A (131 + 1 bunches, 400 + 50 mA) : 33 W,
- Hybrid B (130 + 1 bunches, 400 + 30 mA) : 19 W.

FABRICATION OF DCCT CHAMBER

The new DCCT chamber was fabricated with the ceramic break optimized as described in the previous section. Figure 3 shows a schematic cross-sectional view of the new DCCT chamber.

The new DCCT chamber is based on a circular duct with an inner diameter of 100 mm, and the ceramic break is arranged at its center. The L-shaped sleeves at both ends of the ceramic break are welded from inside the duct. The longitudinal withstand voltage after welding were confirmed to be 2000 M Ω or more for a DC voltage of 1000 V. The dis-

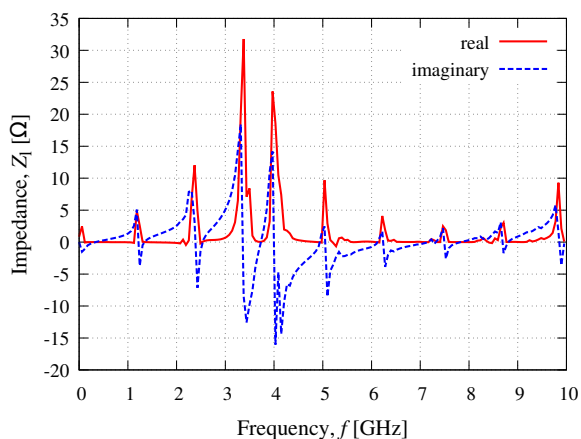


Figure 2: Longitudinal coupling impedance of the ceramic break with final dimensions of $L = 5$ mm, $T = 6$ mm. The inner diameters of the beam duct and cavity space were increased to 100 mm and 200 mm, respectively.

tance between the ICF152 flanges on both ends of the duct is 360 mm. The material of the duct and flanges contacting the vacuum is SUS316L, whereas many of the other parts are made of aluminum alloys for weight reduction. Water-cooling pipes made of oxygen-free copper were bent annularly and attached on the metal sleeves of the ceramic break to efficiently remove the heat generated by the beam power loss. The gap between the cooling pipes and the sleeves was filled with thermally conductive cement to enhance the cooling efficiency. A sheet-like capacitive structure, which was also considered in the beam simulation, was fitted around the ceramic break. The capacitive structure was composed of 50- μ m-thick Kapton film and 100- μ m-thick copper foil and disposed immediately above the ceramic break via Kapton film for insulation. In this case, although the length of the capacitive structure is required to be 46 mm or longer to satisfy the condition of Eq. (1), it was actually limited to 34 mm due to a shortage in the flat surface. This length corresponds to the capacitance of 7.4 nF. The actual capacitance was measured by a precision LCR meter before and after the capacitive structure was attached as 38.7 pF and 1.64 nF, respectively. The value before attachment is almost the same as the expectation if stray capacitances around the ceramic break are considered; however, the value after attachment is approximately one-fourth of the ideal value. Although this difference may be caused by a structural imperfection of the capacitor, no additional measures were performed because DCCT chambers with the same order capacitance as ours have been used without any problems in the PF-AR and SuperKEKB storage rings. The DCCT core with an inner diameter of 175 mm (Bergoz Instrumentation, NPCT-175-RHC020-HR-H) was fixed on a cylindrical pedestal provided outside of the capacitive structure. The fitting tolerance between the core and the pedestal was adjusted carefully so as not to apply any stress to the core. The pedestal is supported in a cantilever from the upstream duct because the upstream and downstream ducts of the ceramic

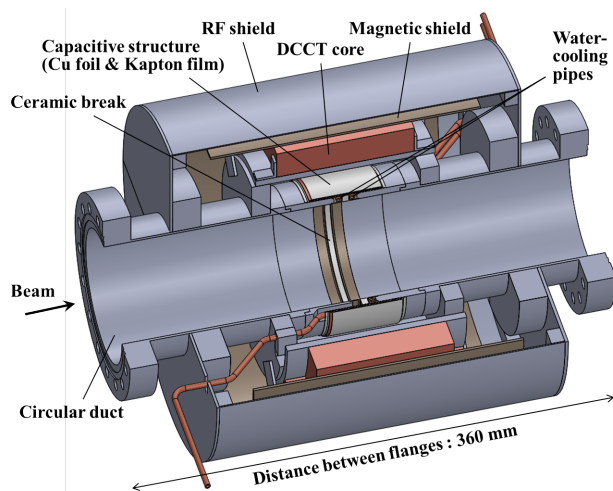


Figure 3: Schematic view of the new DCCT chamber.

break must not be short-circuited inside of the core. Two insulated resistance thermometers were mounted on the capacitive structure contacting the ceramic break and on the pedestal contacting the core to measure the chamber temperature during beam operation. On the exterior of the core, a cylindrical magnetic shield, made of permalloy for shielding an external magnetic field, was disposed. The outermost diameter, thickness, and length of the magnetic shield are 240 mm, 2 mm, and 200 mm, respectively. All of these components were surrounded with a grounded RF shield made of aluminum alloy, which is disposed for shielding the HOMs emitted from the stored beam. This RF shield also plays the important role of bypassing the low-frequency component of the wall current to the exterior of the core. The outermost diameter, thickness, and length of the RF shield are 260 mm, 1 mm, and 260 mm, respectively. The shield is divided into several parts so that it can be easily assembled, and it has a hole to insert the output cable of the core at the upstream end plate.

This new DCCT chamber was assembled offline and installed in the straight section downstream of the RF acceleration cavities located in the northwest of the PF-ring during the 2018 summer shutdown. On just the upstream side of the chamber, a bellows duct with an RF contact having an inner diameter of 100 mm was connected to prevent mechanical stress from being applied to the ceramic break. On the downstream side, a transition duct to convert the circular duct with an inner diameter of 100 mm into a flat duct for quadrupole magnets was connected. Because the taper angle of the inner surface reaches as large as 17° due to limited space, the corresponding heat generation was predicted. According to the GdfidL simulation, the loss factor of this transition duct was estimated to be 41 mV/pC, which was nearly three times that of the ceramic break; therefore, a copper water-cooling jacket covered it. A part of the jacket is also covered on the downstream flange of the DCCT chamber to reduce the heat input. The DCCT chamber and the transition duct were supported by a common frame with an

Content from this work may be used under the terms of the CC BY 3.0 licence (© 2019). Any distribution of this work must maintain attribution to the author(s), title of the work, publisher, and DOI

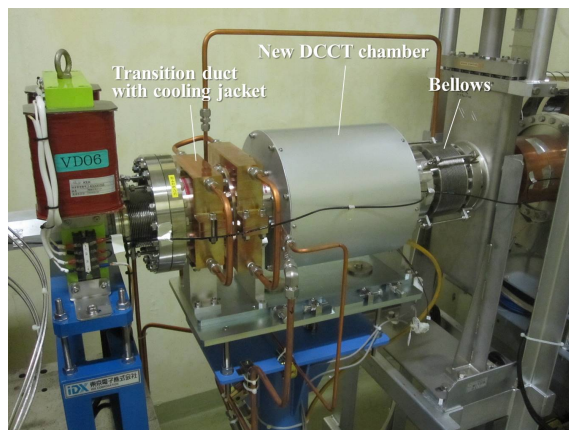


Figure 4: Photo of the new DCCT chamber.

alignment mechanism. Figure 4 is a photo of the new DCCT chamber installed in the PF-ring.

The output signal of the DCCT core is input to the detection circuit installed outside of the radiation shield via a 20-m-long radiation-resistant cable. The output signal of the detection circuit is branched into two signals and read respectively by means of two digital multimeters (DMMs) having different resolution and measurement speed (Keysight Technologies, 34461A and 3458A). Conversion to the stored beam current and correction of a DC offset are performed in the control program for the DMMs. The measured stored current is used not only in the interlock system for machine protection but also for calculations of the beam lifetime and beam injection rate.

EXPERIMENT WITH STORED BEAM

Figure 5 shows the stored beam current measured by the new DCCT in the hybrid filling pattern that will be accompanied by a large power loss and the temperature variation of the chamber measured simultaneously at the two points mentioned above. The DCCT output signal was corrected at zero current and calibrated with a 100-mA test current in advance. The hybrid filling pattern was generated by the control system, which selects the next injection bucket based on measurement results of each bunch current, and maintained by a 5-Hz top-up injection [7].

It can be confirmed by focusing on a flattop part of the measured stored current that a good resolution and time response sufficient to distinguish each injected beam have been obtained. The typical resolution is evaluated to be less than 5 μ A RMS. The measured current exhibits no obvious difference for different filling patterns, and they also agree well with that of the reliable sub-DCCT. The new DCCT chamber can derive the original performance of the core successfully.

The temperature measured in the vicinity of the ceramic break has a faster time response than that measured around the DCCT core because the ceramic break is close to the water-cooling pipes and there is no delay due to heat conduction. The equilibrium temperatures at the ceramic break

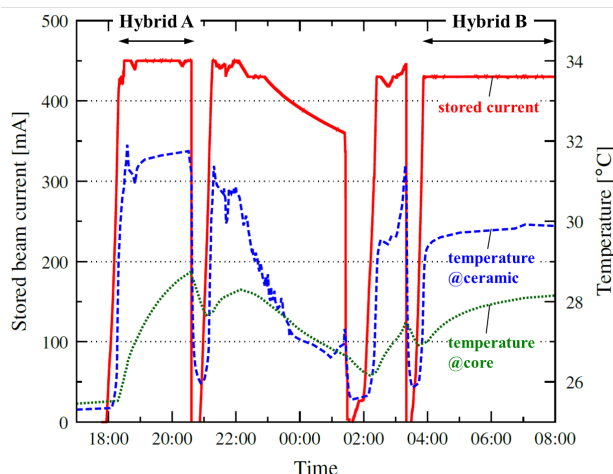


Figure 5: Stored beam current measured by the new DCCT and temperatures at two different points on the chamber.

and DCCT core were 31.8 $^{\circ}$ C and 28.6 $^{\circ}$ C for the filling pattern of Hybrid A, 29.9 $^{\circ}$ C and 28.2 $^{\circ}$ C for that of Hybrid B, and nearly the same value of 25.3 $^{\circ}$ C and 25.4 $^{\circ}$ C with no beams, respectively. Furthermore, they decrease to 26.9 $^{\circ}$ C and 26.6 $^{\circ}$ C for the 450-mA Multibunch filling pattern sharing the most operation time. These temperatures are sufficiently lower than 80 $^{\circ}$ C, which is the maximum operating temperature of the DCCT core. It was demonstrated that the optimum design and cooling mechanism of the ceramic break function effectively to suppress the chamber heating.

Although trends of the temperature variation of the DCCT chamber for different filling patterns agree with the power-loss estimations shown at the end of the design section, their quantitative evaluation remains to be addressed.

SUMMARY

The DCCT consisting of the toroidal core, signal detection circuit and dedicated vacuum chamber has been renewed for the PF-ring. A cylindrical ceramic break was adopted to the new DCCT chamber, and its geometry was optimized considering the beam simulation results and some technical limitations. To suppress the radiation of unneeded HOMs, both ends of the ceramic break was short-circuited by a capacitive structure made of thin Kapton film and copper foil. Water-cooling pipes were also equipped on the metal sleeves at both ends of the ceramic break to suppress chamber heating. The new DCCT was installed in the PF-ring during the 2018 summer shutdown and has been used without any problems since then. The temperature of the new DCCT chamber rises only 6 $^{\circ}$ C, even for a filling pattern including a 50-mA isolated bunch.

ACKNOWLEDGEMENTS

The authors would like to thank M. Arinaga for providing much valuable information on DCCTs for the SuperKEKB storage rings.

REFERENCES

- [1] K. B. Unser, “Beam current transformer with DC to 200 MHz range”, *IEEE Trans. Nucl. Sci.*, NS-16, pp. 934–938, Jun. 1969.
- [2] <http://www.bergoz.com/npct>
- [3] *New Parametric Current Transformer User’s Manual*, Bergoz Instrumentation, Rev. 1.1.
- [4] T. Honda, Y. Hori, and M. Tadano, “Suppression of bunched beam induced heating at the DCCT toroid”, in *Proc. EPAC’98*, Stockholm, Sweden, Jun. 1998, pp. 1526–1528.
- [5] M. Arinaga *et al.*, “KEKB beam instrumentation systems”, *Nucl. Instr. Meth.*, A 499, pp. 100–137, 2003.
- [6] <http://www.gdfidl.de/>.
- [7] R. Takai *et al.*, “Test of hybrid fill mode at the Photon Factory storage ring”, in *Proc. IPAC’10*, Kyoto, Japan, May 2010, pp. 2564–2566.